Method for Connection of Two G^2 Data Sets by the Use of a Quintic Rational Bézier Curve Defined with Mass Control Points

LIONEL GARNIER[1], JEAN-PAUL BÉCAR[2], LAURENT FUCHS[3]

[1]L.I.B., Université de bourgogne, B.P. 47870, 21078 Dijon Cedex, FRANCE
[2]U.P.H.F. - Campus Mont Houy - 59313 Valenciennes Cedex 9, FRANCE
[3]X.L.I.M., U.M.R. 7252, University of Poitiers, FRANCE

Abstract: The paper deals with the G^2 continuity for planar curves. The G^2 continuity is considered as a superior quality of curvature, which is often sought after in high-precision designs and industrial applications. It ensures a perfectly smooth transition between different parts of a surface or curve, which can improve the functionality, aesthetics, and durability of the finished object. This article describes an algorithm to achieve a G^2 junction between two sets of data –point, tangent, curvature–. The junction is based on a rational Bézier curve defined by control mass points. The control mass points generalize those of classical Bézier curves defined with weighted points with no negative weights. It is necessary as vectors and points with negative weights are coming out while applying homographic parameter change on a curve segment or converting any polynomial function into a rational Bézier representation. Here, from two sets of data –point, tangent and curvature–, a Bézier curve of degree n is built. This curve is described by control mass points. In most situations, the best degree for G^2 connection of those two sets equals 5.

Key-Words: Mass points, Rational Quadratic and Quintic Bézier curves, G^2 joints, osculating circle.

Received: June 26, 2024. Revised: November 9, 2024. Accepted: December 4, 2024. Published: December 31, 2024.

1 Introduction

Bézier curves are the simplest control point curves. They were invented in the same time by [1], at Renault and, [2], at Citroën. Initially, any point of these curves is the barycentric locus of a list of weighted points called control points. These points are weighted by Bernstein polynomials, [3], [4], [5]. In case of the sum of the weights equals zero, the barycenter no more exists, [6], [7], [8]. The result of the calculation provides a vector. The solution that generalizes the notion of barycenter consists in using mass points, [9], [10]. Based on this concept and the help of a homographic parameter change, it is possible to determine any conic feature, [11]. This is impossible by using the concept of projective geometry, [12]. Furthermore, this model is independent of the metric or pseudo-metric structure. This model can be used in the Minkowski-Lorentz space to represent canal surfaces, [13].This model offers also to construct Dupin cyclides as subdivided surfaces, [14].Here, the paper deals with the G^2 continuity. The joints are built from a rational Bézier curve with mass control points. The G^2 continuity is considered as a superior quality of curvature, which is often sought after in high-precision designs and industrial applications, such as the production of three-dimensional objects like molds or automotive parts. It ensures a perfectly smooth transition between different parts of a surface or curve, which can improve the functionality, aesthetics, and durability of the finished object. In lighting, G^2 geometric continuity can be applied to the design of reflectors or lenses that are used to control the distribution of light emitted by a light source.

In [15], a parametric cubic spline interpolation scheme for planar curve is given for the construction of $\mathcal{C}^1$ bicubic parametric spline surfaces. They are a generalization of any standard Hermite interpolation. The Pythagorean Hodograph curves were introduced in [16], [17]. In [18], the arc splines that are triarcs interpolate, match unit tangents and curvatures at the interpolation points. In [19], the G^2 blend can be achieved by the curve defined by a pair of polynomial spiral segments. In [20], the G^2 blend is composed of cubic Bézier spirals. In [21], the G^2 blend is built from a quartic rational curve obtained by an inversion of a hyperbola. In [22], the inversion is applied to an arc of spiral. In [23], a cubic rational Bézier spiral (planar curves of monotonic cur-

vature) interpolates end conditions that are positions, tangents and curvatures.

In [24], using complex numbers, the use of Pythagorean-Hodograph quintics of monotone curvature defined in [25], is simplified. In [26], the G^2 blend is computed using planar interpolation with minimum strain energy. For a G^2 conncetion, in [27], one circle is inside the other circle. In [28], a Pythagorean-Hodograph Bézier curve, which is not always a spiral, is used. In [29], the G^2 join is built using curvature variation minimization. In [30], the G^2 join is built with at most spiral segments. In [31], the authors deal with the reachable regions for a single segment of parametric rational cubic Bézier spiral. These curves are computed from the given G^2 Hermite data. This article focuses on the G^2 junction between two curves using Bézier curve of degree n defined by mass control points. Mainly, a quintic rational Bézier curve of that type is one anwer. In our construction, in addition to the G^2 junction, we can enhace the $\mathcal{C}^2$ junction, meaning that velocity is taken into account at the endpoints. When both degenereted circles are straight lines, the null vector $\overrightarrow{0}$ can be used to decrease the degree of the Bézier curve.

The section 2 details the background of mass points and rational Bézier curve with mass control points.

After a presentation of some results on differential properties - tangent vector and curvature- of any rational Bézier curve with control mass points at $t = 0$ and $t = 1$, the section 3, provides a method for G^2 joints. This method takes two sets of G^2 data -point, tangent and curvature for input and returns the mass control points of a Bézier curve of degree 5 for output. The section 4 gives some application examples of the method. A G^2 connection between a circle and a straight line is proposed. In some situation, the curve degree may be down to 4. An example of a G^2 connection between to circles is detailed. Two straight lines are also G^2 connected by the use of the algorithm. The section ends with the joints first G^2 and $\mathcal{C}^1$ and second G^2 et $\mathcal{C}^2$ doing a connection between a Bernouilli Lemniscate loop and a Descartes Folium as they present particular examples: some control mass-point are vectors, including the null vector. Conclusion and perspectives are given in section 5.

2 Rational Bézier curves in $\widetilde{\mathcal{P}}$

In the following $(O;\overrightarrow{\imath};\overrightarrow{\jmath})$ denotes a direct reference frame in the usual Euclidean affine plane $\mathcal{P}$ and $\overrightarrow{\mathcal{P}}$ is the set of vectors of the plane. The set of mass points is defined by

$$\widetilde{\mathcal{P}} = (\mathcal{P} \times \mathbb{R}^*) \cup \left(\overrightarrow{\mathcal{P}} \times \{0\}\right)$$

On the mass point space, the addition, denoted $\oplus$, is defined as follows

- $\omega \neq 0 \Longrightarrow (M;\omega) \oplus (N;-\omega) = \left(\omega\ \overrightarrow{NM};0\right)$;
- $\omega\,\mu\,(\omega+\mu) \neq 0 \implies (M;\omega) \oplus (N;\mu) = \left(\text{Bar}\left\{(M;\omega);(N;\mu)\right\};\omega+\mu\right)$ where $\text{Bar}\left\{(M;\omega);(N;\mu)\right\}$ denotes the barycenter of the weighted points $(M;\omega)$ and $(N;\mu)$;
- $(\overrightarrow{u};0) \oplus (\overrightarrow{v};0) = (\overrightarrow{u}+\overrightarrow{v};0)$;
- $\omega \neq 0 \Longrightarrow (M;\omega) \oplus (\overrightarrow{u};0) = \left(\mathcal{T}_{\frac{1}{\omega}\overrightarrow{u}}(M);\omega\right)$ where $\mathcal{T}_{\overrightarrow{W}}$ is the translation of $\mathcal{P}$ of vector $\overrightarrow{W}$.

In the same way, on the space $\widetilde{\mathcal{P}}$, the multiplication by a scalar, denoted $\odot$, is defined as follows

- $\omega\,\alpha \neq 0 \Longrightarrow \alpha \odot (M;\omega) = (M;\alpha\,\omega)$
- $\omega \neq 0 \Longrightarrow 0 \odot (M;\omega) = \left(\overrightarrow{0};0\right)$
- $\alpha \odot (\overrightarrow{u};0) = (\alpha\overrightarrow{u};0)$

One can note that $\left(\widetilde{\mathcal{P}},\oplus,\odot\right)$ is a vector space, [9], [10], [11]. So, a mass point is a weighted point (M,ω) with $\omega \neq 0$ or a vector $(\overrightarrow{u},0)$.

The Bernstein polynomials of degree n

$$B_{i,n}(t) = \left(\begin{array}{c} n \\ i \end{array}\right)(1-t)^{n-i}\ t^i$$

define rational Bézier curve of degree n.

Definition 1 [Rational Bézier curve (BR curve) in $\widetilde{\mathcal{P}}$]

Let $(P_i;\omega_i)_{i\in[\![0;n]\!]}$ $n+1$ mass points in $\widetilde{\mathcal{P}}$.

Define two sets

$$I = \{i \mid \omega_i \neq 0\} \quad \text{and} \quad J = \{i \mid \omega_i = 0\}$$

Define the weight function ω_f as follows

$$\begin{array}{rccc} \omega_f: & [0;1] & \longrightarrow & \mathbb{R} \\ & t & \longmapsto & \omega_f(t) = \displaystyle\sum_{i\in I} \omega_i \times B_i(t) \end{array}$$

A mass point $(M;\omega)$ or $(\overrightarrow{u};0)$ lays to the rational Bézier curve defined by the control mass points $(P_i;\omega_i)_{i\in[\![0;n]\!]}$ if there is a real t_0 in $[0;1]$ such that:

- if $\omega_f(t_0) \neq 0$ then

$$\left\{\begin{array}{rcl} \omega = & \omega_f(t_0) & \\ \overrightarrow{OM} = & \frac{1}{\omega}\left(\sum_{i\in I}\omega_i B_i(t_0)\,\overrightarrow{OP_i}\right) & \\ & + \quad \frac{1}{\omega_f(t_0)}\left(\sum_{i\in J} B_i(t_0)\,\overrightarrow{P_i}\right) & \end{array}\right. \tag{1}$$

- if $\omega_f(t_0) = 0$ then

$$\overrightarrow{u} = \sum_{i\in I}\omega_i B_i(t_0)\,\overrightarrow{OP_i} + \sum_{i\in J} B_i(t_0)\,\overrightarrow{P_i}$$

Such a curve is denoted $BR\left\{(P_i;\omega_i)_{i\in[\![0;n]\!]}\right\}$

Using $\oplus$ and $\odot$, the mass point $(M;\omega)$ is written as

$$(M;\omega) = \sum_{i\in I\cup J}^{\oplus} B_i(t)\odot(P_i;\omega_i)$$

where $\sum_{i\in I\cup J}^{\oplus}$ denotes a sum of $\oplus$.

If $J = \emptyset$, this definition leads to the usual rational Bézier curve.

3 Method to build a G^2 junction curve

The section highlights some tools used to compute control mass points of the junction curve. The k-level line of a determinant and formal expressions of velocity and curvature are applied in the G^2 building method. All calculation are detailed in the Appendix.

3.1 Tools

3.1.1 The k-level line for a determinant

The following result is used for the computation of the control points.

Proposition 1 : Considering a determinant

$$\det(\overrightarrow{u},\overrightarrow{v})$$

of two vectors $\overrightarrow{u}$ and $\overrightarrow{v}$, if one is fixed, we get a function of the other vector whose k-level curves are straight lines.

Proof : Let $(0,\vec{\imath},\vec{\jmath})$ be an orthoromal frame, k a real number and $M(x,y)$ a point in the plane such that $\det\left(\vec{\imath},\overrightarrow{OM}\right) = k$. Then,

$$\det\left(\vec{\imath},\overrightarrow{OM}\right) = \det(\vec{\imath},y\vec{\jmath}) = y = k$$

Conversely, any point of the straight line passing by H such that $\overrightarrow{OH} = k\vec{\jmath}$ and directed by $\vec{\imath}$ is convenient, see Figure 1.

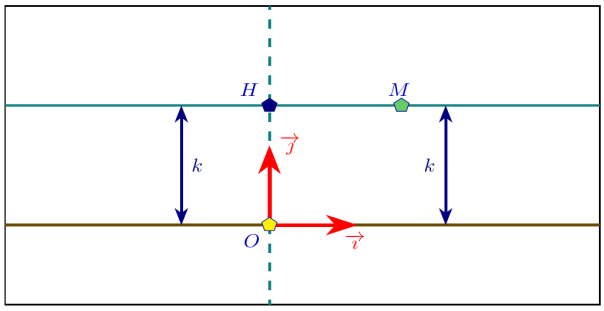

Figure 1: k-level line of a determinant.

3.1.2 Curvature and joints

Definition 2 (a curve curvature)

Let γ be a plane curve defined by a regular $\mathcal{C}^2$ parametrisation γ. The curvature $\rho(t_0)$ in a point $\gamma(t_0)$ of γ satisfies

$$\rho(t_0) = \frac{\left|\det\left(\frac{\overrightarrow{d\gamma}}{dt}(t_0);\frac{\overrightarrow{d^2\gamma}}{dt^2}(t_0)\right)\right|}{\left\|\frac{\overrightarrow{d\gamma}}{dt}(t_0)\right\|^3}$$

The osculating circle to a curve γ, at a point M_0 where the curvature not vanishes is the best approximation, [7], [32], of curve arc in the neighbourhood of M_0. It is the only tangent circle to γ at M_0 possessing three common points with γ. The curvature radius $R(t_0)$ equals the inverse of curvature $\rho(t_0)$ to this curve at that point.

If the curvature $\rho(t_0)$ equals zero thus the curvature radius $R(t_0)$ is equal to infinity. It implies that the center of osculating circle is moved at infinity, [33]. In the case of $\frac{\overrightarrow{d^2\gamma}}{dt^2}(t_0)$ is non-collinear to $\frac{\overrightarrow{d\gamma}}{dt}(t_0)$, the osculating curvature center $\Omega(t_0)$ at $M_0 = \gamma(t_0)$ is given by

$$\overrightarrow{M_0\Omega(t_0)} = R(t_0)\,\overrightarrow{n^p}(t_0)$$

where $\overrightarrow{n^p}(t_0)$ is the main unit normal vector to γ at point $\gamma(t_0)$ witch verifies

$$\overrightarrow{n^p}(t_0)\bullet\frac{\overrightarrow{d^2\gamma}}{dt^2}(t_0) > 0$$

Definition 3 (geometrical joint)

Let γ_0 and γ_1 be two plane curves respectively defined on $[a;b]$ and $[c;d]$.

the geometrical joint between γ_0 and γ_1 is:

- G^0 if $\gamma_0(b) = \gamma_1(c)$;
- G^1 if $\gamma_0(b) = \gamma_1(c)$ and $\overrightarrow{\frac{d\gamma_0}{dt}}(b) = \lambda\overrightarrow{\frac{d\gamma_1}{dt}}(c)$, with $\lambda \in \mathbb{R}^*$, thus the curve share the same tangent line at the contact point;
- G^2 if the joint is G^1 $\rho_{\gamma_0}(b) = \rho_{\gamma_1}(c)$ and $\overrightarrow{n^{p'}_{\gamma_0}}(t_0) = \overrightarrow{n^{p'}_{\gamma_1}}(t_0)$ thus the curve share the same osculating circle at the contact point.

3.1.3 Velocity, acceleration and curvature at $t = 0$ for a rational Bézier curve with mass control points

Let n be an integer greater or equal to 3. Let ω_0 be non null real number. Let γ be Bézier curve with control mass points $(P_0;\omega_0)$, $(P_1;\omega_1)$, $\cdots$, $(P_n;\omega_n)$.

Let us define the function χ by

$$\begin{array}{rccc} \chi: & \mathbb{R} & \longrightarrow & \mathbb{R}^* \\ & 0 & \longmapsto & 1 \\ & t & \longmapsto & t \end{array} \tag{2}$$

For any k, the vector $\widetilde{P_k} = \overrightarrow{P_0P_k}$ if $\omega_k \neq 0$ or $\widetilde{P_k} = \overrightarrow{P_k}$ if $\omega_k = 0$, using the function of Formula (2), the equation (1) is thus written

$$\widetilde{M_0} = \frac{1}{\sum_{k=0}^{n} \omega_k B_{k,n}(t)} \sum_{k=1}^{n} \chi(\omega_k) B_{k,n}(t) \widetilde{P_k}$$

with $\widetilde{M_0} = \overrightarrow{P_0M}$ if $\sum_{k=0}^{n} \omega_k B_{k,n}(t) \neq 0$ and $\widetilde{M_0} = \overrightarrow{M_0}$ otherwise.

Velocity at $t = 0$

If $\omega_1 = 0$ the velocity at $t = 0$ equals

$$\frac{n}{\omega_0}\overrightarrow{P_1}$$

If $\omega_1 \neq 0$ the velocity at $t = 0$ equals

$$n\frac{\omega_1}{\omega_0}\overrightarrow{P_0P_1}$$

Curvature at $t = 0$

The acceleration vector at $t = 0$ equals

$$\begin{array}{rcl} \overrightarrow{\frac{d^2\overrightarrow{P_0\gamma}}{dt^2}}(0) & = & 2n\left(\frac{\omega_0 - n\omega_1}{\omega_0^2}\right)\chi(\omega_1)\widetilde{P_1} \\ & + & \frac{1}{\omega_0}n(n-1)\chi(\omega_2)\widetilde{P_2} \end{array} \tag{3}$$

The curvature $\rho(0)$ at $t = 0$ is given by

$$\left| \frac{\omega_0(n-1)\chi(\omega_2)\det\left(\frac{1}{\left\|\widetilde{P_1}\right\|}\widetilde{P_1};\widetilde{P_2}\right)}{n\chi(\omega_1)^2\left\|\widetilde{P_1}\right\|^2} \right|$$

The curvature at $t = 0$ equals zero if

$$\det\left(\widetilde{P_1};\widetilde{P_2}\right) = 0$$

3.1.4 Velocity, acceleration and curvature at $t = 1$ for a rational Bézier curve with mass control points

Let ω_0 be non null real number. Let γ be Bézier curve with mass control points $(P_0;\omega_0)$, $(P_1;\omega_1)$, $\cdots$, $(P_n;\omega_n)$.

Let define $\widetilde{P_k} = \overrightarrow{P_nP_k}$ if $\omega_k \neq 0$ and $\widetilde{P_k} = \overrightarrow{P_k}$ if $\omega_k = 0$, using the function of Formula (2), the Equation (1) is written

$$\widetilde{M_n} = \frac{1}{\sum_{k=0}^{n} \omega_k B_{k,n}(t)} \sum_{k=0}^{n} \chi(\omega_k) B_{k,n}(t) \widetilde{P_k}$$

with $\widetilde{M_n} = \overrightarrow{P_nM}$ if $\sum_{k=0}^{n} \omega_k B_{k,n}(t) \neq 0$ and $\widetilde{M_n} = \overrightarrow{M_n}$ otherwise.

Velocity at $t = 1$

- if $\omega_{n-1} = 0$, the velocity at P_n is given by
$$\frac{d}{dt}\overrightarrow{O\gamma(1)} = -\frac{n}{\omega_n}\overrightarrow{P_{n-1}}$$
- if $\omega_1 \neq 0$, the velocity at P_n is given by
$$\frac{d}{dt}\overrightarrow{O\gamma(1)} = -n\frac{\omega_{n-1}}{\omega_n}\overrightarrow{P_nP_{n-1}}$$

The acceleration vector at $t = 1$ is given by

$$\begin{array}{rcl} \overrightarrow{\frac{d^2\overrightarrow{P_n\gamma}}{dt^2}}(1) = & -2n\left(\frac{\omega_n - n\omega_{n-1}}{\omega_n^2}\right)\chi(\omega_{n-1})\widetilde{P_{n-1}} \\ & + & \frac{1}{\omega_n}n(n-1)\chi(\omega_{n-2})\widetilde{P_{n-2}} \end{array}$$

Curvature at $t = 1$

Let n be an integer greater or equal to 3. Let ω_0 be a non null real number. Let γ be Bézier curve with control mass points $(P_0;\omega_0)$, $(P_1;\omega_1)$, $\cdots$, $(P_n;\omega_n)$

The curvature $\rho(1)$ at $t = 1$ equals

$$\left| \frac{\alpha_n \ \det\left(\frac{1}{\left\| \widetilde{P_{n-1}} \right\|} \widetilde{P_{n-1}}; \widetilde{P_{n-2}} \right)}{n\chi(\omega_{n-1})^2 \left\| \widetilde{P_{n-1}} \right\|^2} \right|$$

where

$$\alpha_n = \omega_n (n-1) \chi(\omega_{n-2})$$

The curvature equals zero if

$$\det\left(\widetilde{P_{n-1}}; \widetilde{P_{n-2}} \right) = 0$$

3.2 Method description

Input:

(P_0, ω_0), (P_1, ω_1) two first mass control points and ρ_0 the curvature at $t = 0$.

(P_{n-1}, ω_{n-1}), (P_n, ω_n) two last mass control points and ρ_1 the curvature at $t = 1$.

Output :

(P_2, ω_2), (P_{n-2}, ω_{n-2}) two mass control points for the Bézier curve of degree n.

Description :

The algorithm provides the two mass control points that define a Bézier curve of degree n that joins the data at $t = 0$ and $t = 1$. The best degree equals 5 otherwise the other mass control points can be arbitrary chosen.

Begin G^2 connection

Step 1 : P_2 computation

Case $\rho_0 \neq 0$

Let us define $\beta_n = \omega_0 (n-1)$.

- if $\omega_1 = \omega_2 = 0$, P_2 satisfies :

$$\rho_0 = \left| \frac{\beta_n \det\left(\frac{1}{\left\| \overrightarrow{P_1} \right\|} \overrightarrow{P_1}; \overrightarrow{P_2} \right)}{n \left\| \overrightarrow{P_1} \right\|^2} \right|$$

- if $\omega_1 \neq 0$ and $\omega_2 = 0$, P_2 satisfies :

$$\rho_0 = \left| \frac{\beta_n \det\left(\frac{1}{\left\| \overrightarrow{P_0P_1} \right\|} \overrightarrow{P_0P_1}; \overrightarrow{P_2} \right)}{n\omega_1^2 \left\| \overrightarrow{P_0P_1} \right\|^2} \right|$$

- if $\omega_1 = 0$ and $\omega_2 \neq 0$, P_2 satisfies :

$$\rho_0 = \left| \frac{\beta_n \omega_2 \det\left(\frac{1}{\left\| \overrightarrow{P_1} \right\|} \overrightarrow{P_1}; \overrightarrow{P_0P_2} \right)}{n \left\| \overrightarrow{P_1} \right\|^2} \right|$$

- if $\omega_1\omega_2 \neq 0$, P_2 satisfies :

$$\rho_0 = \left| \frac{\beta_n \omega_2 \det\left(\frac{1}{\left\| \overrightarrow{P_0P_1} \right\|} \overrightarrow{P_0P_1}; \overrightarrow{P_0P_2} \right)}{n\omega_1^2 \left\| \overrightarrow{P_0P_1} \right\|^{2`}} \right|$$

case $\rho_0 = 0$

- if $\omega_1 = \omega_2 = 0$, both vectors $\overrightarrow{P_1}$ and $\overrightarrow{P_2}$ are collinear vectors.
- if $\omega_1 \neq 0$ and $\omega_2 = 0$, the vector $\overrightarrow{P_2}$ equals $\overrightarrow{0}$ or a direction vector of the straight line (P_0P_1).
- if $\omega_1 = 0$ and $\omega_2 \neq 0$, the vector $\overrightarrow{P_1}$ a direction vector of the straight line (P_0P_2).
- if $\omega_1\omega_2 \neq 0$, the points P_0, P_1 and P_2 lay on a same straight line.

Step 2 : P_{n-2} calculation

Case $\rho_1 \neq 0$

Let us define

$$\delta_n = \omega_n (n-1)$$

and

$$\sigma_n = \omega_n (n-1) \omega_2$$

- if $\omega_{n-1} = \omega_{n-2} = 0$,

$$\rho_1 = \left| \frac{\delta_n \det\left(\frac{1}{\left\| \overrightarrow{P_{n-1};} \right\|} \overrightarrow{P_{n-1}}; \overrightarrow{P_{n-2}} \right)}{n \left\| \overrightarrow{P_{n-1}} \right\|^2} \right|$$

- if $\omega_{n-1} \neq 0$ and $\omega_{n-2} = 0$

$$\rho_1 = \left| \frac{\det\left(\frac{\delta_n}{\left\| \overrightarrow{P_nP_{n-1}} \right\|} \overrightarrow{P_nP_{n-1}}; \overrightarrow{P_{n-2}} \right)}{n\omega_{n-1}^2 \left\| \overrightarrow{P_nP_{n-1}} \right\|^2} \right|$$

- if $\omega_1 = 0$ and $\omega_2 \neq 0$,

$$\rho_1 = \left| \frac{\det\left(\frac{\sigma_n}{\left\| \overrightarrow{P_{n-1}} \right\|} \overrightarrow{P_{n-1}}; \overrightarrow{P_n P_{n-2}} \right)}{n \left\| \overrightarrow{P_{n-1}} \right\|^2} \right|$$

- if $\omega_{n-1}\omega_{n-2} \neq 0$,

$$\rho_1 = \left| \frac{\det\left(\frac{\sigma_n}{\left\| \overrightarrow{P_n P_{n-1}} \right\|} \overrightarrow{P_n P_{n-1}}; \overrightarrow{P_n P_{n-2}} \right)}{n\omega_{n-1}^2 \left\| \overrightarrow{P_n P_{n-1}} \right\|^2} \right|$$

Case $\rho_1 = 0$

- if $\omega_{n-1} = \omega_{n-2} = 0$, the vectors $\overrightarrow{P_{n-1}}$ and $\overrightarrow{P_{n-2}}$ are collinear vectors.
- if $\omega_{n-1} \neq 0$ and $\omega_{n-2} = 0$, the vector $\overrightarrow{P_{n-2}}$ equals $\overrightarrow{0}$ or a direction vector of the line $(P_n P_{n-1})$.
- if $\omega_{n-1} = 0$ and $\omega_{n-2} \neq 0$, the vector $\overrightarrow{P_{n-1}}$ is one direction vector of the line $(P_n P_{n-2})$.
- if $\omega_{n-1}\omega_{n-2} \neq 0$, the points P_n, P_{n-1} and P_{n-2} lay on the same straight line.

End G2 connection
Proof :
For any integer $k \geq 3$, and $\omega_0 \neq 0$, $\widetilde{P_k}$ is defined as follows:

- if $\omega_k \neq 0$ then $\widetilde{P_k} = \overrightarrow{P_0 P_k}$;
- if $\omega_k = 0$ then $\widetilde{P_k} = \overrightarrow{P_k}$.

In the case of a non null curvature, P_2 is calculated from

$$\rho_0 = \left| \frac{\omega_0 (n-1) \chi(\omega_2) \det\left(\widetilde{P_1}; \widetilde{P_2} \right)}{n \chi(\omega_1)^2 \left\| \widetilde{P_1} \right\|^3} \right|$$

otherwise from

$$\det\left(\widetilde{P_1}; \widetilde{P_2} \right) = 0$$

The four cases are coming out from the definition of the χ function. The algorithm returns the six points (P_i, ω_i) where $i \in \{0, 1, 2, n-2, n-1, n\}$ as output data where n equals the rational Bézier curve degree. The lower degree can be obtained when the next control mass point P_3 starting from P_0 equals P_{n-2} thus $n = 5$.

From Formula (3.2), it yields

$$\det\left(\frac{1}{\left\| \widetilde{P_1} \right\|^3} \widetilde{P_1}; \widetilde{P_2} \right) = \frac{\rho_0 \, n \, \chi(\omega_1)^2 \left\| \widetilde{P_1} \right\|^2}{(n-1) \, \omega_0 \, \chi(\omega_2)}$$

and the computation of $\widetilde{P_2}$ depends on the curvature ρ_0 of the circle, the weights ω_0, ω_1 and ω_2, the degree n of the curve and the norm of the vector $\widetilde{P_1}$.

4 Examples

4.1 G^2 joints between two circles

In this example, both circles match their osculating circle at any point of the circles. The input data are a circle, a point of the circle and a point of the tangent line at the previous point of the circle. The first set is composed by the points $P_0(-2, 2)$, $P_1(-1, 2)$ and $\rho_0 = \frac{4}{9}$ see the magenta circle on Figure 2. The second set is composed by the points $P_5(3, -1)$, $P_4(3, 0)$ and $\rho_1 = \frac{4}{3}$ see the red circle on Figure 2. All weights are fixed to 1.

The algorithm computes $P_2(0, 3)$ and $P_3(2, 0)$. The weight ω_i where $i \in [\![0, 5]\!]$ can be chosen for the mass control points P_0, P_1, P_2, P_3, P_4 and P_5. They define the quintic Bézier curve in blue on Figure 2 that G^2 connects both circles.

4.2 G^2 joints between a ciruclar arc and a straight line

In this case, the circle arc matches the osculating circle at any point of the arc. At any point of a straight line the curvature of a straight line equals zero as the radius of curvature is infinity. The first set of data are defined by P_0 on the circle arc, P_1 on the tangent line to the circle at P_0. The curvature ρ_0 equals the inverse of the radius arc. The second set of data is composed by the two points P_4 and P_5 and a null curvature ρ_1 at P_5. The particular situation offers the choice of all weights ω_i, $i \in [\![0, 5]\!]$. After computing the points P_2 and P_3, the algorithm achieves the control points $(P_i; \omega_i)$, $i \in [\![0, 5]\!]$.
Detailed data for the Figure 3.

1. At $t = 0$, the curvature is $\rho_0 = \frac{\sqrt{2}}{2}$ and the control mass points are given in the Table 1;
2. At $t = 1$, the curvature is $\rho_1 = 0$ and the control mass points are given in the Table 2.

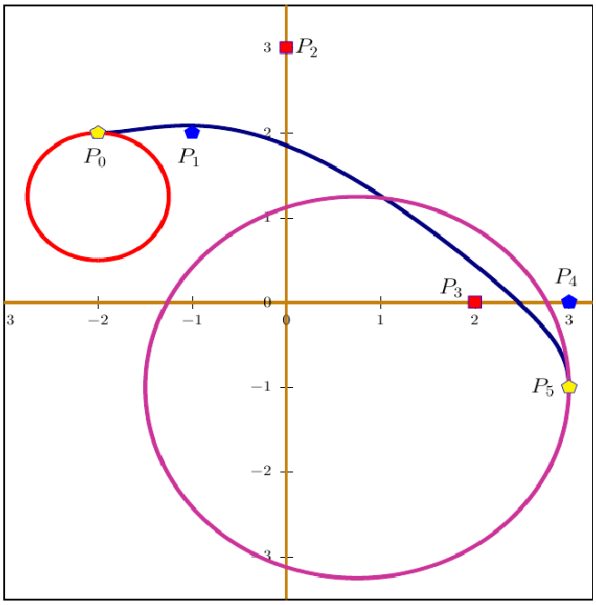

Figure 2: G^2 blends between two circles by a rational Bézier curve of degree 5.

Table 1: Control mass points of the rationel Bézier curve in Figure 3 at $t = 0$.

Point	$P_0\,(1,-1)$	$P_1\,(3,1)$	$P_2\left(\frac{43}{16},\frac{21}{16}\right)$
Weight	$\omega_0 = 2$	$\omega_1 = \frac{1}{2}$	$\omega_2 = 2$

Table 2: Control mass points of the rationel Bézier curve in Figure 3 at $t = 1$.

Point	$P_3\left(\frac{9}{2},\frac{3}{2}\right)$	$P_4\,(4,1)$	$P_5\,(3,0)$
Weight	$\omega_3 = 2$	$\omega_4 = 3$	$\omega_5 = 1$

The circle arc is defined by the equation:

$$\gamma_0(t) = \left(\sqrt{2}\cos(t)\,;\sqrt{2}\sin(t)\right),\ t \in \left[\frac{3\pi}{4};\frac{7\pi}{4}\right]$$

The two points P_0 and P_1 satisfy $P_0 = \gamma_0\left(\frac{7\pi}{4}\right)$ and $P_1 = P_0 + 2\frac{\overrightarrow{d\gamma_0}}{dt}\left(\frac{7\pi}{4}\right)$. The point H defined in the preamble equals $H\left(\frac{11}{16},-\frac{11}{16}\right)$.

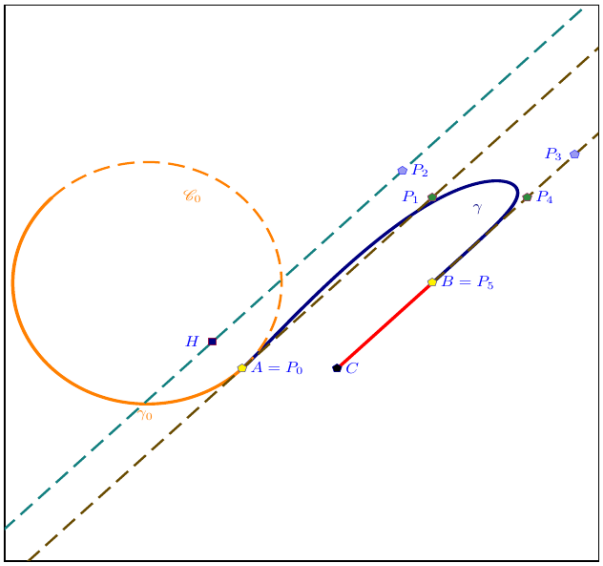

Figure 3: G^2 joints between a half of circle and a segment based on a quintic rational Bézier curve

4.3 G^2 joints between a circle arc and a straight line changing weights

$P_0\,(-2;2)$, $P_1\,(-1;2)$ and $\rho_0 = \frac{1}{2}$ are chosen. The Figure 4 shows the position of the line (HP_2) changing the weights, see Table 3 which gives the coordinates of the point H. The other points are $P_3\left(\frac{5}{2};1\right)$, $P_4\left(\frac{11}{4};1\right)$ and $P_5\,(3;1)$ and the other weights value equals 1.

Table 3: The position of the point H depends on the weight ω_0, ω_1 and ω_2, see Figure 4.

ω_0	ω_1	ω_2	H
1	1	1	$(-2;2.625)$
2	3	2	$\left(-2;\frac{109}{32}=3.40625\right)$
1	2	1	$\left(-2;\frac{9}{2}\right)$

The same result is obtained at $t = 1$.

4.4 G^2 joints between half a circle and a segment based on a quartic rational Bézier curve

In the Figure 5 the straight line defined by H and $\overrightarrow{P_0P_1}$ cuts the segment $[P_5P_4]$.

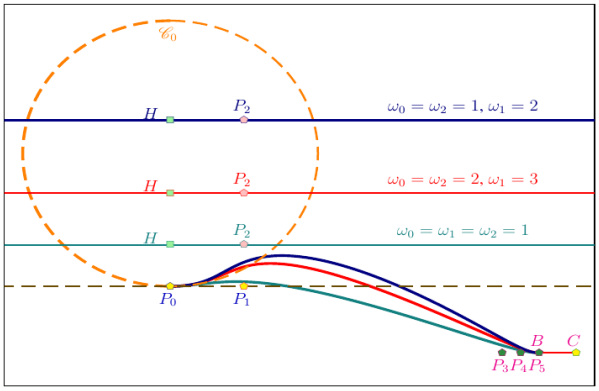

Figure 4: Three G^2 blends with Bézier curves with several values of weights.

The choice of $P_2 = P_3$ at the intersection makes the curve degree down to 4. From the input data $P_0\,(1,-1))$, $\omega_0 = 2$, $P_1\,(3,1))$, $\omega_0 = 0.5$, $\rho_0 = \frac{\sqrt{2}}{2}$ $P_4\,(3,0))$, $\omega_4 = 3$, $P_5\,(3,-1))$, $\omega_5 = 1$, $\rho_1 = 0$, the algorithm provides $H\,(\frac{2}{3},-\frac{2}{3}))$, $P_2\,(3,\frac{5}{3})$ and $P_3 = P_2$.

4.5 G^2 joints on two parallel segments

Five mass control points defining a quartic can be chosen. A null vector is added in the Bézier representation.

In the Figure 6 the parallel lines are G^2 connected by a quartic curve. A mass control point is replaced by a null vector. $P_0\,(1,1)$, $\omega_0 = 1$, $P_1\,(1,0)$, $\omega_1 = 1$, $\overrightarrow{P_2} = \overrightarrow{0}$, $\omega_2 = 0$, $P_3\,(2,0)$, $\omega_3 = 1$, $P_4\,(2,-1)$ and $\omega_4 = 1$.

The data for the Figure 7 follow $P_0\,(1,1)$, $\omega_0 = 1$, $\overrightarrow{P_1}\,(0,-\frac{1}{2})$, $\omega_1 = 0$, $\overrightarrow{P_2} = \overrightarrow{0}$, $\omega_2 = 0$, $\overrightarrow{P_3}\,(0,\frac{1}{2})$, $\omega_3 = 0$, $P_4\,(2,-1)$ and $\omega_4 = 1$.

These results can be used to define tube connections. As illustrated on Figure 8 and Figure 9 where the tubes are revolution surfaces obtained from the curves of Figure 6 and Figure 7.

4.6 G^2 between a loop of Descartes Folium and a Bernouilli Lemniscate.

4.6.1 Bézier representation of both loops

On the Figure 10 the Lemniscate loop γ_P is modeled by the five mass control points: $(P_0;1)$, $\left(\overrightarrow{P_1};0\right)$, $\left(\overrightarrow{P_2};0\right)$, $\left(\overrightarrow{P_3};0\right)$, $(P_4;1)$ with $P_0\,(-\frac{1}{2};0)$, $\overrightarrow{P_1}\,(-\frac{1}{4};-\frac{1}{4})$, $\overrightarrow{P_2}\,(0;0)$, $\overrightarrow{P_3}\,(-\frac{1}{4};\frac{1}{4})$ and $P_4 = P_0$ applying the translation of vector $-\frac{1}{2}\overrightarrow{\imath}$.

On the same Figure, the Descartes folium loop γ_Q is modeled by a rational Bézier cubic with the following mass control points : $Q_0\,(0;2)$, $\omega_{Q_0} = 1$,

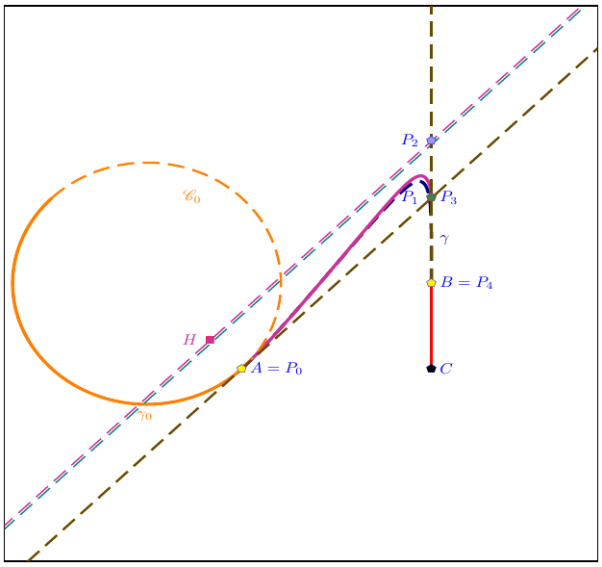

Figure 5: G^2 between the half-circle γ_0 and the segment $[BC]$ by a rational quartic Bézier curve γ.

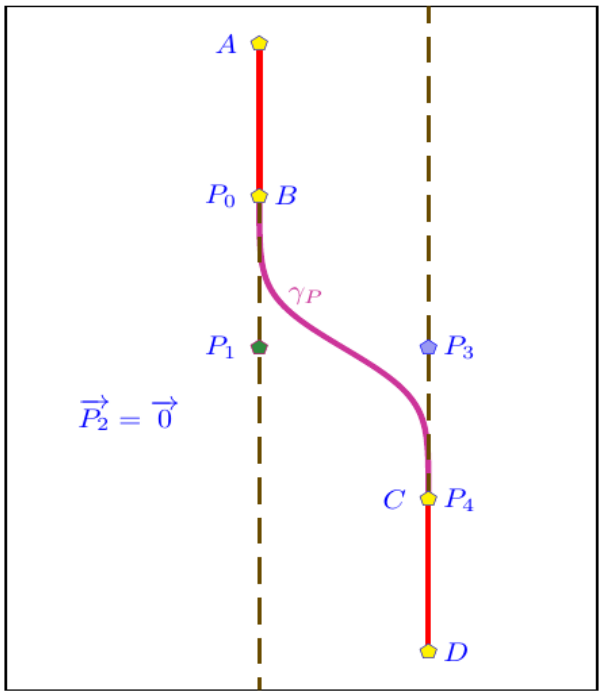

Figure 6: G^2 blends between two parallel segments by a quartic rational Bézier curve: four control points and the control null vector.

$\overrightarrow{Q_1}\,(2;0)$, $\omega_{Q_1} = 0$, $\overrightarrow{Q_2}\,(0;2)$, $\omega_{Q_2} = 0$, and $Q_3 = Q_0$, $\omega_{Q_3} = 1$, applying the translation of vector

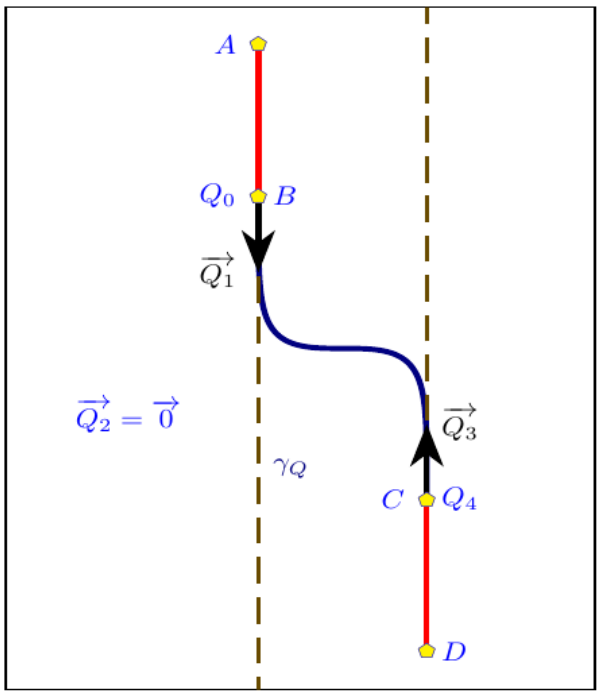

Figure 7: G^2 blends between two parallel segments by a quartic rational Bézier curve: two control points, two control non-null vectors and the control null vector.

Figure 8: Two G^2 blends using a lathe from the curve in the Figure 6.

$\frac{1}{2}\overrightarrow{\imath} + 2\overrightarrow{\jmath}$.

The Bézier representation of the two loops is used to compute their osculating circles at the given points that are P_4 for γ_P and Q_0 for γ_Q. As $\overrightarrow{P_2} = \overrightarrow{0}$, the curvature at P_4 equals zero. The curvature at Q_0 equals $\rho_1 = \frac{1}{3}$.

The connecting curve denoted γ_R is a Bézier quintic curve with mass control points (R_i, ω_i), $i \in [\![0, 5]\!]$, defined by $R_0 = Q_0$, $\omega_0 = 2$, $\overrightarrow{R_1}\left(\frac{2}{5}, \frac{2}{5}\right)$, $\omega_1 = 0$, $R_2\left(\frac{3}{2}; -2\right)$, $\omega_2 = 1$, $R_3\left(-1; \frac{7}{3}\right)$, $\omega_3 = 1$, $\overrightarrow{R_4}\left(-\frac{6}{5}, 0\right)$, $\omega_4 = 0$, $R_5 = P_5$, $\omega_5 = 1$. The Figure 11 shows a G^2 and $\mathcal{C}^1$ connection between the loop of lemniscate γ_P and the loop of the folium γ_Q by a quintic Bézier curve γ_R and both osculating circles.

4.6.2 Finding $\mathcal{C}^2$ connection for two loops

The quintic rational Bézier curve doing the G^2 connection between the loop of Descartes folium and one loop of Bernouilli lemniscate is built from the six mass control points (S_i, ω_i) with $i \in [\![0, 5]\!]$. In case of a $\mathcal{C}^2$ connection is necessary, the method can also be used to compute it. Freeing S_2, S_3 provides a G^1 or $\mathcal{C}^1$ at most. Then, $S_0\left(\frac{1}{2}, 2\right) = Q_3$, $\omega_0 = 2$, $S_1\left(\frac{1}{2}, -\frac{2}{5}\right)$, $\omega_1 = 1$, $S_2\left(\frac{17}{10}, \frac{14}{10}\right)$, $\omega_2 = 1$, $S_3\left(\frac{3}{10}, \frac{4}{5}\right)$, $\omega_3 = 1$, $S_4\left(-\frac{2}{5}, \frac{1}{10}\right)$, $\omega_4 = 2$, $S_5\left(-\frac{1}{2}, 0\right) = P_0$ and $\omega_5 = 1$. The Figure 12 shows a G^2 joints to $\mathcal{C}^2$ connection between both loops and also osculating circles.

Figure 13 shows a future application of G^2-continuity to handwriting modeling.

5 Conclusion and perspectives

The paper has shown a method that computes a Bézier curve that G^2 connects two sets of data. Each set of data is composed by a given tangent line and a given curvature at the given point. The connection curve is at least a quintic rational curve defined by mass control points that are weighted points with any type of weight. In the case of a null weight a vector is obtained. The article shows that the G^2 connection offers two degree of freedom. For a $\mathcal{C}^1$ connection, there is one degree of freedom left. There is no more degree of freedom for a $\mathcal{C}^2$ connection implying only a unique solution. The results perform a handwriting modelling by the use of that type of Bézier curve. The thick and thin strokes of handwriting is an application. Further applications are on the way of the 3d do-

Figure 9: Two G^2 blends using a lathe from the curve in the Figure 7.

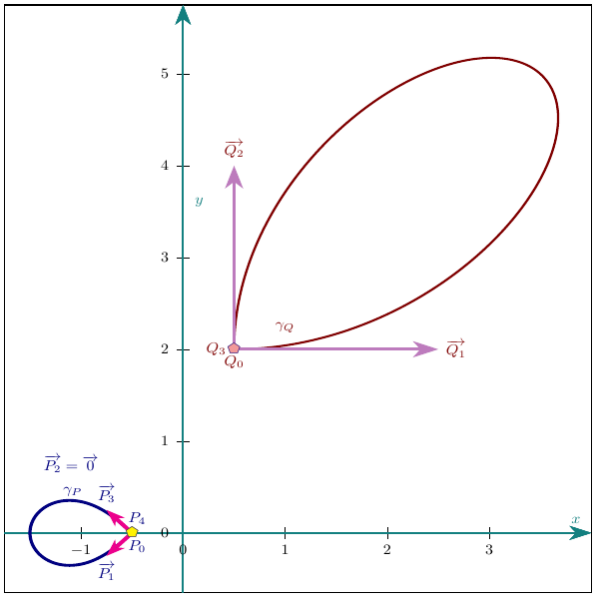

Figure 10: Two loops for G^2 connection

main as the torsion of space curves based on the Frenet frame.

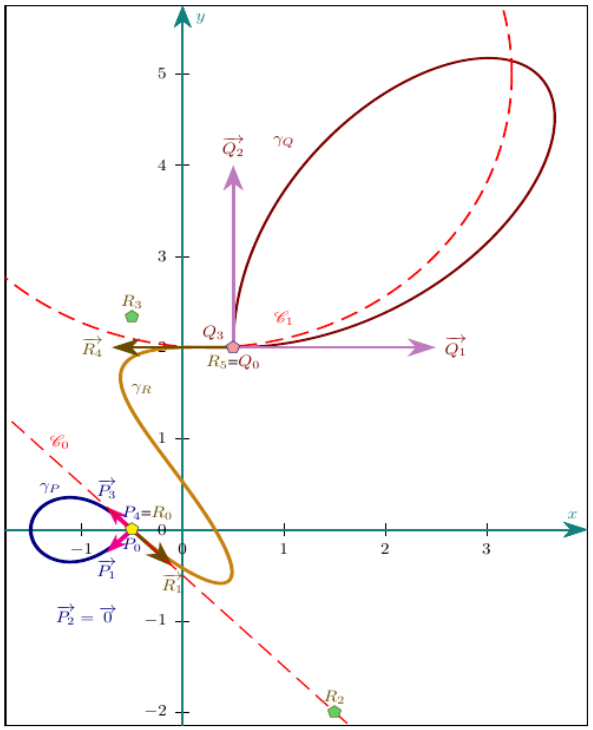

Figure 11: A quintic Bézier rational curve connecting G^2 and $\mathcal{C}^1$ beween the loop of Descartes folium and a loop a Bernouilli lemniscate

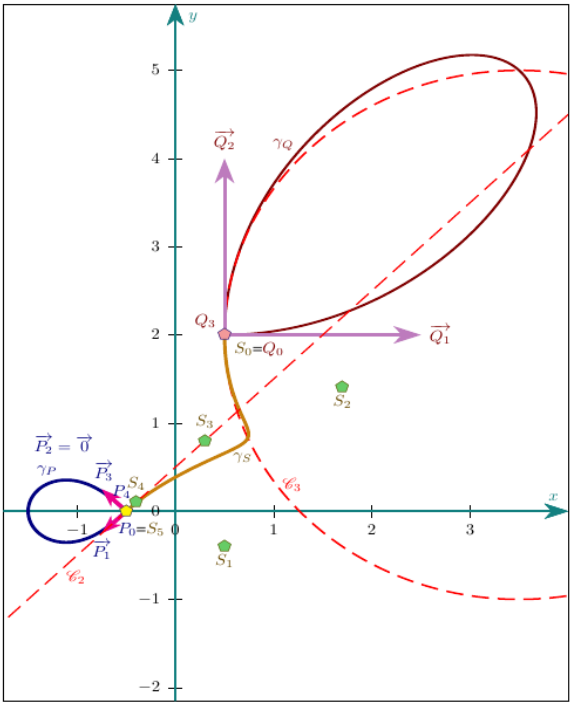

Figure 12: A quintic Bézier rational curve connecting G^2 and $\mathcal{C}^2$ beween the loop of Descartes folium and a loop a Bernouilli lemniscate

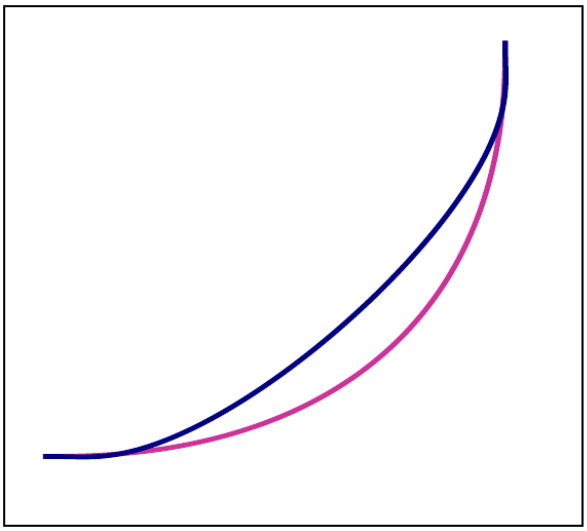

Figure 13: G^2 connection between a quartic Bézier curve and a quintic Bézier curve to model the thick and thin strokes of handwriting.

References:

[1] P. Bézier. Courbe et surface, volume 4. Hermès, Paris, 2ème edition, Octobre 1986.

[2] P. De Casteljau. Mathématiques et CAO. Volume 2 : formes à pôles. Hermes, 1985.

[3] Gerald Farin. From conics to nurbs: A tutorial and survey. IEEE Comput. Graph. Appl., 12(5):78–86, September 1992.

[4] G. Farin. NURBS from Projective Geometry to Pratical Use. A K Peters, Ltd, 2 edition, 1999. ISBN 1-56881-084-9.

[5] L. Piegl and W. Tilles. A managerie of rational b-spline circles. IEEE Computer Graphics and Applications, 9(5):46–56, 1989.

[6] M. Gourion. Mathématiques, Terminales C et E, tome 2. Fernand Nathan, 1983.

[7] Y. Ladegaillerie. Géométrie pour le CAPES de Mathématiques. Ellipses, Paris, 2002. ISBN 2-7298-1148-6.

[8] Y. Ladegaillerie. Géométrie affine, projective, euclidienne et anallagmatique. Ellipses, Paris, 2003. ISBN 2-7298-1416-7.

[9] J. C. Fiorot and P. Jeannin. Courbes et surfaces rationnelles, volume RMA 12. Masson, 1989.

[10] J. C. Fiorot and P. Jeannin. Courbes splines rationnelles, applications à la CAO, volume RMA 24. Masson, 1992.

[11] Lionel Garnier and Jean-Paul Bécar. Mass points, Bézier curves and conics: a survey. In Eleventh International Workshop on Automated Deduction in Geometry, Proceedings of ADG 2016, pages 97–116, Strasbourg, France, June 2016. http://ufrsciencestech.u-bourgogne.fr/∼garnier/publications/adg2016/.

[12] L.A. Piegl and W. Tiller. The NURBS book. Monographs in visual communication. Springer, 1995.

[13] Lionel Garnier, Jean-Paul Bécar, and Lucie Druoton. Canal surfaces as Bézier curves using mass points. Computer Aided Geometric Design, 54:15–34, 2017.

[14] Lionel Garnier, Lucie Druoton, Jean-Paul Bécar, Laurent Fuchs, and Géraldine Morin. Subdivisions of Ring Dupin Cyclides Using Bézier Curves with Mass Points. WSEAS TRANSACTIONS ON MATHEMATICS, 20:581–596, 11 2021.

[15] Carl de Boor, Klaus Höllig, and Malcolm Sabin. High accuracy geometric hermite interpolation. Computer Aided Geometric Design, 4(4):269–278, 1987.

[16] R. T. Farouki and T. Sakkalis. Pythagorean hodographs. IBM Journal of Research and Development, 34(5):736–752, 1990.

[17] Rida T. Farouki. 1. Pythagorean—Hodograph Curves in Practical Use, pages 3–33.

[18] D.S. Meek and D.J. Walton. Planar osculating arc splines. Computer Aided Geometric Design, 13(7):653–671, 1996.

[19] D.J. Walton and D.S. Meek. G2 curve design with a pair of pythagorean hodograph quintic spiral segments. Computer Aided Geometric Design, 24(5):267–285, 2007.

[20] D.J. Walton and D.S. Meek. G2 curves composed of planar cubic and pythagorean hodograph quintic spirals. Computer Aided Geometric Design, 15(6):547–566, 1998.

[21] A.I. Kurnosenko. Two-point g2 hermite interpolation with spirals by inversion of hy-

perbola. Computer Aided Geometric Design, 27(6):474–481, 2010.

[22] A. Kurnosenko. Applying inversion to construct planar, rational spirals that satisfy two-point g2 hermite data. Computer Aided Geometric Design, 27(3):262–280, 2010.

[23] Donna A. Dietz, Bruce Piper, and Elena Sebe. Rational cubic spirals. Computer-Aided Design, 40(1):3–12, 2008. Constrained Design of Curves and Surfaces.

[24] Rida T Farouki. Pythagorean-hodograph quintic transition curves of monotone curvature. Computer-Aided Design, 29(9):601–606, 1997.

[25] Desmond J. Walton and Dereck S. Meek. A pythagorean hodograph quintic spiral. Comput. Aided Des., 28:943–950, 1996.

[26] Lizheng Lu. Planar quintic g2 hermite interpolation with minimum strain energy. Journal of Computational and Applied Mathematics, 274:109–117, 2015.

[27] Zulfiqar Habib and Manabu Sakai. On ph quintic spirals joining two circles with one circle inside the other. Computer-Aided Design, 39(2):125–132, 2007.

[28] Zulfiqar Habib and Manabu Sakai. Transition between concentric or tangent circles with a single segment of g2 ph quintic curve. Computer Aided Geometric Design, 25(4):247–257, 2008. Pythagorean-Hodograph Curves and Related Topics.

[29] Lizheng Lu, Chengkai Jiang, and Qianqian Hu. Planar cubic g1 and quintic g2 hermite interpolations via curvature variation minimization. Computers and Graphics, 70:92–98, 2018. CAD/Graphics 2017.

[30] Zulfiqar Habib and Manabu Sakai. G2 cubic transition between two circles with shape control. Journal of Computational and Applied Mathematics, 223(1):133–144, 2009.

[31] Zulfiqar Habib and Manabu Sakai. Admissible regions for rational cubic spirals matching g2 hermite data. Computer-Aided Design, 42(12):1117–1124, 2010.

[32] M. Berger and B. Gostiaux. Géométrie différentielle : variétés, courbes et surfaces. PUF, 2ème edition, avril 1992.

[33] M. Audin. Géométrie. EDP Sciences, 2006. ISBN 2-86883-883-9.

Appendix

A Proof of Formula (3)

From the relation

$$\begin{aligned}\overrightarrow{P_0\gamma(t)} &= \chi(\omega_1)\, n\, t\,(1-t)^{n-1}\,\widetilde{P_1} \\ &+ \chi(\omega_2)\,\frac{n(n-1)}{2}\,t^2\,(1-t)^{n-2}\,\widetilde{P_2} \\ &+ \sum_{k=3}^{n}\chi(\omega_i)\,B_{k,n}(t)\,\widetilde{P_k}\end{aligned}$$

the velocity vector is equal to

$$\begin{aligned}&\frac{d}{dt}\overrightarrow{P_0\gamma(t)} \\ =\ & \chi(\omega_1)\, n\left((1-t)^{n-1} - t(n-1)(1-t)^{n-2}\right)\widetilde{P_1} \\ +\ & \chi(\omega_1)\,\frac{n(n-1)}{2}\left(2t(1-t)^{n-2}\right)\widetilde{P_1} \\ +\ & \chi(\omega_1)\,\frac{n(n-1)}{2}\left(-t^2(n-2)(1-t)^{n-3}\right)\widetilde{P_1} \\ +\ & \sum_{k=3}^{n}\chi(\omega_i)\,\frac{d}{dt}B_{k,n}(t)\,\widetilde{P_k}\end{aligned}$$

The acceleration vector is computed as follows

$$\begin{aligned}&\frac{d^2\overrightarrow{P_0\gamma(t)}}{dt^2} \\ =\ & -\frac{d''(t)\,d(t) - 2\left(d'(t)\right)^2}{\left(d(t)\right)^3}\overrightarrow{P0\gamma(t)} \\ -\ & 2\frac{d'(t)}{\left(d(t)\right)^2}\,\frac{d}{dt}\overrightarrow{P_0\gamma(t)} + \frac{1}{d(t)}\,\frac{d^2}{dt^2}\overrightarrow{P_0\gamma(t)}\end{aligned} \tag{4}$$

and the acceleration vector is simplified to

$$\begin{aligned}&\frac{d^2}{dt^2}\overrightarrow{P_0\gamma(t)} \\ =\ & \chi(\omega_1)\, n(n-1)\left(-(1-t)^{n-2}\right)\widetilde{P_1} \\ -\ & \chi(\omega_1)\, n(n-1)\left((1-t)^{n-2} + t(1-t)^{n-3}\right)\widetilde{P_1} \\ +\ & \chi(\omega_2)\,\frac{n(n-1)}{2}\left(2(1-t)^{n-2}\right)\widetilde{P_2} \\ +\ & \chi(\omega_2)\,\frac{n(n-1)}{2}\left(-2(n-2)\,t(1-t)^{n-2}\right)\widetilde{P_2} \\ +\ & \chi(\omega_2)\,\frac{n(n-1)}{2}\left(-2t(n-2)(1-t)^{n-3}\right)\widetilde{P_2} \\ +\ & \chi(\omega_2)\,\frac{n(n-1)}{2}t^2(n-2)(n-3)(1-t)^{n-4}\,\widetilde{P_2} \\ +\ & \sum_{k=3}^{n}\chi(\omega_i)\,\frac{d^2}{dt^2}B_{k,n}(t)\,\widetilde{P_k}\end{aligned}$$

which, at $t=0$ leads to

$$\left\{\begin{array}{rcl}\overrightarrow{P_0\gamma(0)} & = & \overrightarrow{0}\\ \frac{d}{dt}\overrightarrow{P_0\gamma(0)} & = & n\chi(\omega_1)\widetilde{P_1}\\ \frac{d^2}{dt^2}\overrightarrow{P_0\gamma(t)} & = & n(n-1)\left(-2\chi(\omega_1)\widetilde{P_1}+\chi(\omega_2)\widetilde{P_2}\right)\end{array}\right.$$

Let $d(t)$ be defined by

$$\begin{array}{rcl}d(t) = & \omega_0(1-t)^n+\omega_1 n\,t(1-t)^{n-1}\\ & + & \omega_2\frac{n(n-1)}{2}t^2(1-t)^{n-2}+\sum_{k=3}^{n}\omega_i B_{k,n}(t)\end{array}$$

and the expression of the first derivative of d is equal to

$$\begin{array}{rcl}& & d'(t)\\ & = & -\omega_0 n(1-t)^{n-1}\\ & + & \omega_1 n\left((1-t)^{n-1}-(n-1)t(1-t)^{n-2}\right)\\ & + & \omega_2\frac{n(n-1)}{2}2t(1-t)^{n-2}\\ & - & \omega_2\frac{n(n-1)}{2}(n-2)t^2(1-t)^{n-3}\\ & + & \sum_{k=2}^{n}\omega_i\frac{d}{dt}B_{k,n}(t)\end{array}$$

and the expression of the second derivative of d equals

$$\begin{array}{rcl}& & d''(t)\\ & = & \omega_0 n(n-1)(1-t)^{n-2}\\ & - & 2\omega_1 n\left((n-1)(1-t)^{n-2}\right)\\ & + & \omega_1 n\left((n-1)\left((n-2)t(1-t)^{n-2}\right)\right)\\ & + & \omega_2 n(n-1)\left((1-t)^{n-2}-t(1-t)^{n-3}\right)\\ & - & \omega_2\frac{n(n-1)}{2}(n-2)\left(2t(1-t)^{n-3}\right)\\ & - & \omega_2\frac{n(n-1)}{2}(n-3)t^2(1-t)^{n-3}\\ & + & \sum_{k=2}^{n}\omega_i\frac{d^2}{dt^2}B_{k,n}(t)\end{array}$$

that leads to

$$\left\{\begin{array}{rcl}d(0) & = & \omega_0\\ d'(0) & = & n(\omega_1-\omega_0)\\ d''(0) & = & n(n-1)(\omega_0-2\omega_1+\omega_2)\end{array}\right.$$

and

$$\begin{array}{rcl}& & \frac{d''(0)d(0)-2(d'(0))^2}{(d(0))^3}\\ & = & \frac{n(n-1)\omega_0(\omega_0-2\omega_1+\omega_2)-2n^2(\omega_1-\omega_0)^2}{\omega_0^3}\\ & = & n\frac{(n-1)(\omega_0-2\omega_1+\omega_2)-2n(\omega_1-\omega_0)^2}{\omega_0^2}\end{array}$$

and

$$\frac{d'(0)}{(d(0))^2} = n\frac{\omega_1-\omega_0}{\omega_0^2}$$

Based on Formula (4), the acceleration vector equals

$$\begin{array}{l}\frac{d^2}{dt^2}\overrightarrow{P_0\gamma(0)}\\ =-2n\frac{\omega_1-\omega_0}{\omega_0^2}n\chi(\omega_1)\widetilde{P_1}\\ +\frac{1}{\omega_0}n(n-1)\left(-2\chi(\omega_1)\widetilde{P_1}+\chi(\omega_2)\widetilde{P_2}\right)\\ =-2n\frac{\omega_1-\omega_0}{\omega_0^2}n\chi\left(\omega_1\widetilde{P_1}\right)\\ +\frac{1}{\omega_0}n(n-1)\left(-2\chi(\omega_1)\widetilde{P_1}+\chi(\omega_2)\widetilde{P_2}\right)\\ =-2n\left(n\frac{\omega_1-\omega_0}{\omega_0^2}+\frac{n-1}{\omega_0}\right)\chi(\omega_1)\widetilde{P_1}\\ +\frac{1}{\omega_0}n(n-1)\chi(\omega_2)\widetilde{P_2}\\ =2n\left(\frac{\omega_0-n\omega_1}{\omega_0^2}\right)\chi(\omega_1)\widetilde{P_1}\\ +\frac{1}{\omega_0}n(n-1)\chi(\omega_2)\widetilde{P_2}\end{array}$$

and four cases must be distinguished for the acceleration vector at P_0:

- if $\omega_1=\omega_2=0$,

$$\frac{d^2}{dt^2}\overrightarrow{P_0\gamma(0)}=\frac{2n}{\omega_0}\overrightarrow{P_1}+n\frac{n-1}{\omega_0}\overrightarrow{P_2}$$

- if $\omega_1\neq 0$ and $\omega_2=0$,

$$\begin{array}{rcl}& & \frac{d^2}{dt^2}\overrightarrow{P_0\gamma(0)}\\ & = & 2n\left(\frac{\omega_0-n\omega_1}{\omega_0^2}\right)\omega_1\overrightarrow{P_0P_1}\\ & + & \frac{1}{\omega_0}n(n-1)\overrightarrow{P_2}\end{array}$$

- if $\omega_1 = 0$ and $\omega_2 \neq 0$, ■

$$\frac{d^2}{dt^2}\overrightarrow{P_0\gamma(0)} = \frac{2n}{\omega_0}\overrightarrow{P_1} + \frac{\omega_2}{\omega_0}n(n-1)\overrightarrow{P_0P_2}$$

- if $\omega_1\omega_2 \neq 0$,

$$\begin{aligned}\frac{d^2}{dt^2}\overrightarrow{P_0\gamma(0)} &= 2n\left(\frac{\omega_0 - n\omega_1}{\omega_0^2}\right)\omega_1\overrightarrow{P_0P_1} \\ &+ \frac{\omega_2}{\omega_0}n(n-1)\overrightarrow{P_0P_2}\end{aligned}$$

Contribution of Individual Authors to the Creation of a Scientific Article (Ghostwriting Policy)
The authors equally contributed in the present research, at all stages from the formulation of the problem to the final findings and solution.

Sources of Funding for Research Presented in a Scientific Article or Scientific Article Itself
No funding was received for conducting this study.

Conflict of Interest
The authors have no conflicts of interest to declare that are relevant to the content of this article.